

Damping in dense gas acoustic structure interaction

J.P.M. Smeulers*, H.P. Pereboom, N. González Díez

TNO Heat Transfer and Fluid Dynamics

*Corresponding author: Leeghwaterstraat 44, 2628 CA Delft, jan.smeulers@tno.nl

Abstract: In centrifugal compressors as applied in the oil and gas industry, pressure pulsations can excite strong vibrations of the impeller leading to failure. Specifically in so-called dense gas compressors, such as carbon dioxide compressors operating at pressures up to 200 bar, these vibrations can be very strong. The strong vibrations are due to Fluid Structure Interaction (FSI). Coupled acoustic structural resonance modes can be excited at the blade passing frequency and multiples. These resonance modes have low damping and can develop in the impeller and diffuser of a compressor stage. The most important resonances are those modes in which a coupling between the high density fluid and the impeller structure occurs.

In a Joint Industry Project (JIP) the occurrence of coupled resonance modes has been investigated both experimentally and by means of modelling. The results of the project show that Fluid Structure Interaction (FSI) has a large effect on the vibration modes of the impeller. It has been shown that the coupled eigen frequencies and modes can be predicted with satisfactory accuracy by means of vibroacoustic COMSOL models. However, the predicted damping of the modes showed large discrepancies with the experiments. It is suspected that the models used for the damping are not adequate. New damping models and additional tests are necessary to accurately develop damping models.

Keywords: FSI, centrifugal compressor, impeller, vibrations, acoustic resonance, acoustic and structural damping, boundary layer absorption model.

1. Introduction

In large centrifugal compressors acoustic resonances can excite vibrations of the impeller that can lead to failure. Especially when an acoustical resonance mode coincides with an excitation frequency (blade passing frequency) and with a structural vibration mode of the impeller, the vibrations can become very strong leading to failure. Therefore in the design of a compressor stage, the objective is to avoid the

coincidence of resonance modes and excitation frequencies. For high density compressors this coincidence cannot be avoided in many cases. This is because the acoustic and structural resonance are coupled due to Fluid Structure Interaction (FSI). If the coupling is strong there are no separate acoustic and structural modes. In that case there is always coincidence of modes. In addition the mode density in the frequency spectrum is large, causing that for any excitation frequency a resonance condition will be encountered. Therefore the design of a high density compressor stage has to be based on the assumption that resonance modes will be excited. Therefore the vibration stresses that will occur at all resonance have to be calculated. This means that both the mode frequencies and shapes and the damping have to be determined accurately.

In 2012 a Joint Industry Project (JIP) has been initiated to develop knowledge about the FSI in centrifugal compressor stages. The project comprised the development of models and experimental validation by means of a test rig. For the modelling, COMSOL has been applied. Multi-physics models have been applied that include an acoustic model of the fluid in the compressor stage that has been coupled with a structural model of the impeller. The static parts of the stage are considered to be infinitely rigid.

A simplified geometry has been investigated consisting of a disk in a narrow cavity. The fluid that has been applied is carbon dioxide (CO₂) with a variable pressure of 50 to 200 bar and a temperature of 60 °C. The resonance modes and frequencies that are predicted by the models comply very well with the measurements. However, the measured damping of the modes does not comply with theory.

In this paper, first a description of a centrifugal compressor stage and the simplified geometry is presented. Next the modelling techniques that have been applied are discussed. The validation results are described as well as possible improvement of modelling of the damping. Conclusions and recommendations are offered at the end of the paper.

2. The dynamics of a centrifugal compressor stage.

A centrifugal compressor often consists of multiple stages as is shown in figure 1. Each stage consists of an impeller, the rotating part, and a static part.

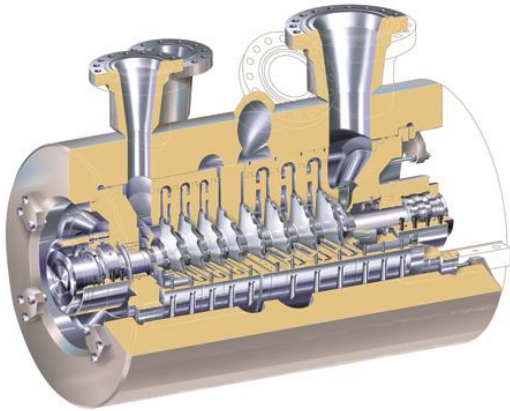


Figure 1 Example of a barrel type centrifugal compressor for high pressure applications.

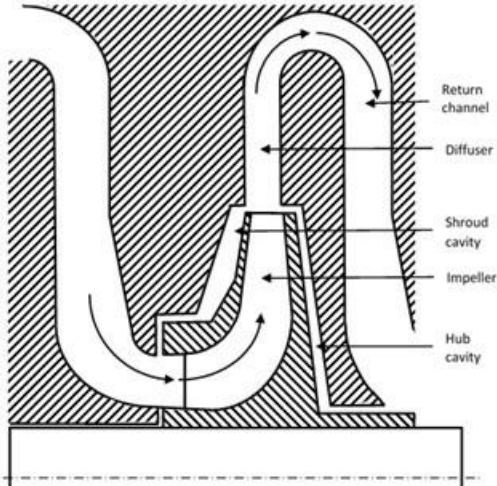


Figure 2 Cross section of a centrifugal compressor stage.

2.1 Geometry and flow path

In figure 2 a cross section of the typical geometry of a centrifugal compressor stage is shown. The impeller has an axial inflow that turns in radial direction towards the impeller exit. The impeller has a number of blades that force the flow in radial

and tangential direction. From the impeller exit the flow enters the diffuser where the flow velocity is reduced and the kinetic energy of the flow gained in the impeller is converted into pressure. From the diffuser the flow makes a U-turn into the return channel leading to the next stage.

The impeller has a circular back plate, the hub, and a cover plate, the shroud. The impeller rotates in a static housing, leaving cavities at the hub and the shroud side. The main flow is passing through the impeller and the diffuser. There is only a small leakage flow through the cavities.

2.2 Acoustic modes

Acoustic resonance modes in the shroud and hub cavities can lead to high pressure pulsations in the compressor internals. A typical example of an acoustic mode is shown in figure 3.

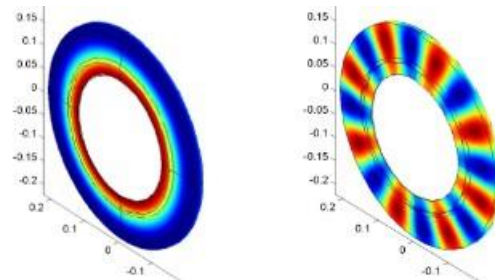


Figure 3 Example of two acoustic modes in a shroud cavity. Left a radial and right a tangential mode.

Depending on the mode shape a resonance mode can induce large vibration forces on the impeller. These can be particularly severe if the resonance modes are combined in the shroud and hub cavities with opposite phase of the pressures on each side.



Figure 4 A typical failure of an impeller due to acoustic excitation.

As the shroud plate is the weakest, a failure as shown in figure 4 will occur in the shroud. A crack will in most cases start at the weld between a blade and the shroud plate.

An acoustic resonance can be excited by flow disturbances generated by the blades of the impeller. Therefore the blade passing frequency (BPF) is the dominant frequency of the excitation. However, also multiples of the BPF occur. The frequency range of interest is in practice 500 to 5000 Hz.

Besides impeller blades in real compressors also other sets of vanes are present. For instance there are vanes in the return channel and sometimes in the diffuser. These vanes may lead to other excitation frequencies that are a linear combination of the number of blades and vanes, the so-called Tyler-Sofrin modes.

2.3 Structural modes

High vibration stresses that can cause failure will occur if a structural resonance of the impeller is excited. In figure 5 an example of a structural mode of an impeller is shown. The vibration mode shows lobes that are similar to an acoustic mode in the cavity.

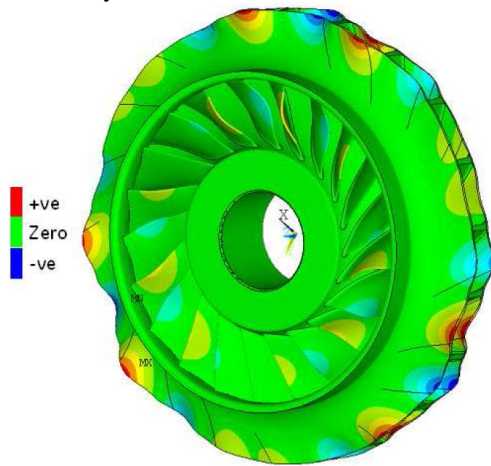


Figure 5 Example of a mode shape of an impeller. Here an 'in plane mode' is shown, i.e. both shroud and hub move in the same direction.

High vibration stresses will happen if an acoustic mode and a structural mode comply, i.e. have (almost) the same frequency and mode shape.

3. Analysis of a centrifugal compressor stage by modelling.

In order to avoid high frequency problems during the design of a compressor stage, the chance on incidence of an acoustical and structural mode with a dominant excitation frequency has to be determined.

3.1 Analysis for low density gases

The typical strategy to avoid problems is to make the difference between the excitation frequencies, the acoustic resonance frequencies and the structural resonance frequencies as large as possible. The usual approach is to calculate the acoustic and structural modes with separate finite element models and check the (triple) coincidence in a coincidence diagram. Without further detail, an example of such a diagram is shown in figure 6.

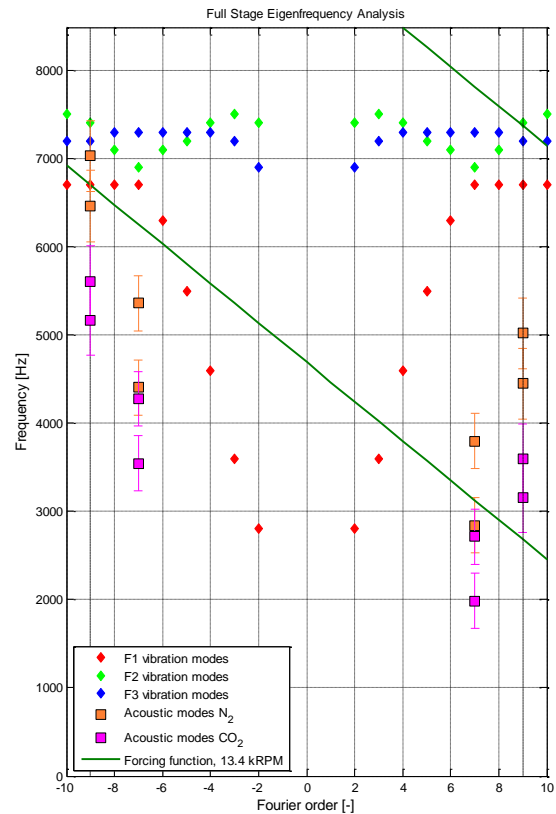


Figure 6 Example of coincidence diagram showing for which conditions a triple coincidence can occur. See reference [1].

3.2 Analysis for dense gas compressors

For dense gas compressors the acoustic and structural modes are coupled. The higher the density the stronger the coupling. The frequency of the modes shifts depending on the density of the gas. At very high densities the difference between acoustic and structural modes disappears completely. On the one hand this simplifies the analysis because there is only need to check the coincidence of one frequency per mode with the excitation frequencies. On the other hand a coupled acoustic-structural mode has to be used to determine the resonance frequencies, which is more complex.

3.3 Development of acoustic-structural models

In a Joint Industry Project (JIP) multi-physics models have been developed to analyze the coupled modes. COMSOL has been used for this. To minimize the complexity, simplified geometries have been used instead of a real compressor stage. The geometry and dimensions of the test specimen have been chosen such that they are comparable with real compressor stages. In figure 7 the model of one of the configurations is shown. In this case the impeller is replaced by a simple disk. Also a specimen consisting of a double disk with 15 blades has been analyzed, which resembles more a real impeller. Several parameters have been varied, such as the depth and width of the cavities, the clearance of the impeller rim with the stator and the opening of the diffuser.

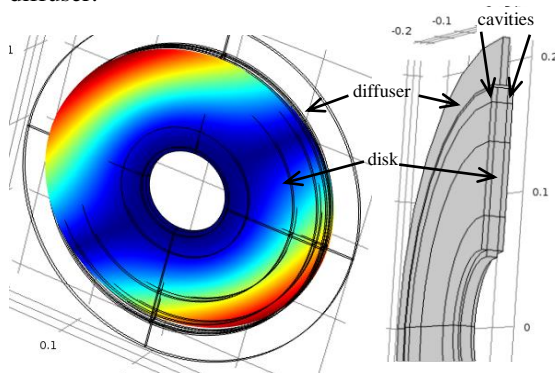


Figure 7 Example of a model of the test configuration with a simple disk. Left: the gas space is transparent (wire frame model). A vibration mode of the disk is shown. Right: a cross section.

The fluid used is pure carbon dioxide (CO_2) at a temperature of approximately 60°C . The pressure has been varied between 50 and 200 bar. By selecting a temperature of 60°C the critical point of CO_2 , i.e. 73.9 bar and 31.1°C , is passed with a safe margin. This is to avoid uncertainties of the density and speed of sound when passing near the critical pressure.

The impeller/disk is not rotating and there is no flow. Therefore the system can be described with a pressure acoustic model for the volume filled with fluid and a linear elastic model for the disk. The acoustic boundaries are all “Sound Hard Boundaries” except for the areas that are in contact with the disk. For these Acoustic-Structure Boundaries have been defined. The disk has been clamped at the inner ring.

An acoustic damping model called Boundary-layer absorption (BLA) model with the wide duct approximation has been applied. This model describes the damping that is caused by the acoustic boundary layer due to viscosity and heat exchange between fluid and walls. The structural damping is very small and is neglected compared with the acoustic damping. See also [3].

A structured quadrilateral mesh has been applied.

3.4 Modelling results

For the evaluation of impeller vibrations firstly the frequency and shapes of the modes are important. Specifically the change of the eigen frequencies as a function of the fluid density is of interest. As a first step the eigen frequencies are calculated for a wide range of pressures.

Secondly also the damping of the vibration modes has to be known, because in most practical cases the excitation of vibration modes cannot be avoided. Therefore the worst case of running at a resonance condition has to be analyzed. For this the damping has to be known.

The calculated eigen frequencies appear to be accurate within 2% except for the lower modes. The reason for this is that for the lower modes the support of the shaft on which the disk is mounted is much weaker than assumed in the model where this support is assumed to be infinitely stiff.

In figure 8 the results of a response calculation are shown (FRFs) as a function of the mean working pressure. For this with the “Frequency-Domain Modal” method has been applied to the model without damping. The frequency of the various modes depends on the density of the fluid, i.e. the

pressure. Therefore the modes are tracked as is shown by the red lines. The frequency of some modes decrease with increasing pressures, others increase, as is expected from theory.

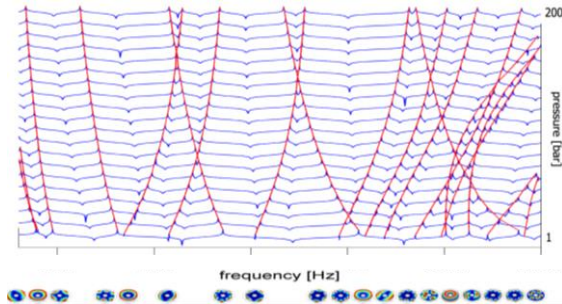


Figure 8 Calculated FRFs for a simple disk as a function of the pressure (blue lines) and tracking of modes (red lines).

As the model includes damping, the eigen values and frequencies are complex numbers. The imaginary part of an eigen frequency, divided by the modulus of the frequency gives the modal damping coefficient for that mode. However, it appeared that this swift way of determining the modal damping does not give reliable results. The modal damping derived in this way appears to be much higher than is derived from the measurements. Moreover, the damping that is derived from the response calculation, described below, is also much smaller. This issue has not been solved so far.

An alternative procedure has been used to determine the damping, i.e. by calculating the response for a large number of frequencies by direct integration. The result is a frequency response function (FRF) that is comparable to the processed measurement results. This method requires (unacceptable) long computation times because the response is calculated for approximately 1000 frequencies and ten mean pressure levels. Calculating the FRF with the “Frequency-Domain Modal” method, which is far more computationally efficient, is not an option, because this method is based on the complex eigen values and mode shapes.

For calculating the FRF the model is excited mechanically with a unit force (1 N amplitude) at the same point as in the test rig. Also an acoustic excitation can be applied, which is a Flow

Monopole Source at exactly the same point where the test specimen is excited in the tests. For both mechanical and acoustic excitation a stepped sine has been applied.

4. Validation with test results

A test rig has been designed and built to validate the models consisting of a vessel with an internal diameter of 500 and a length of 1000 mm. See figure 10.



Figure 9 Test vessel with in the front the quick opening and closing door.

In the vessel various impeller configurations can be tested with CO₂ at 60 °C and in a pressure range of 50 to 200 bar.

Two types of impeller configurations have been tested: the simple disk and the “generic impeller” consisting of two disks with blades in between. See figure 10.

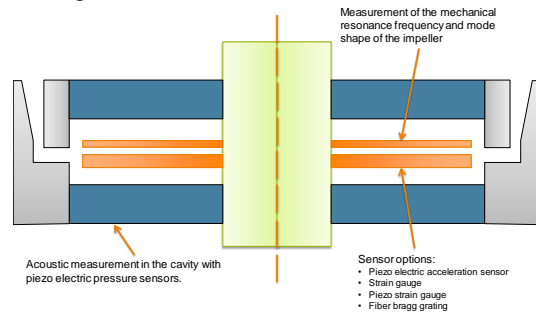


Figure 10 The “generic impeller” configuration. Two circular plates (orange) with blades in between. The blue and grey parts represent the stator and diffuser.

The two excitation mechanisms that have been used are shown in figure 11.

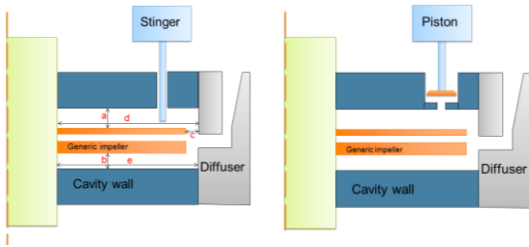


Figure 11 Excitation mechanisms. Left the mechanical excitation by means of a pulse. Right the acoustic excitation by means of an oscillating piston.

Figure 12 shows the “Generic Impeller” with a large number of strain gauges used to determine the mode shapes. In addition also an accelerometer has been mounted on the impeller, which has better signal to noise properties. More details about the test set-up can be found in [2].

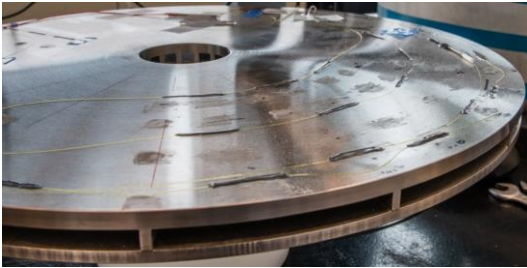


Figure 12 The “Generic Impeller” equipped with a large number of optical fibre strain gauges.

The processed measurement results, i.e. the FRFs, as is shown in figure 13 comply well with the predictions of the model. The shift of the resonance frequencies complies well with the predictions.

At relatively low frequencies, lower than 1000 Hz, separate modes can be identified. In the region encircled in red the modes cannot be separated anymore. The mode density is high in that range, which means that at any frequency a vibration mode can be excited.

In figure 14 the eigen frequencies have been extracted from the FRFs.

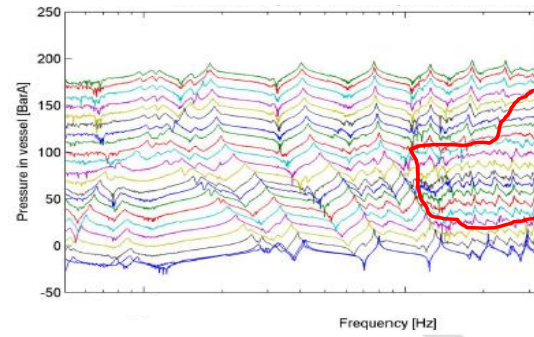


Figure 13 Measured FRFs (Frequency Response Functions) as a function of the mean pressure. Pulse excitation by the stinger; response measured by an accelerometer.

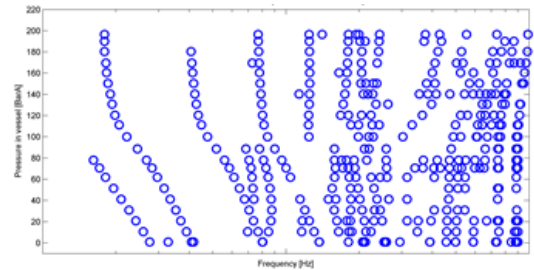


Figure 14 Logarithmic x-axis response of “Simple Disk” configuration.

Besides comparing the frequencies of resonance peaks also the vibration modes should be compared in order to unambiguously compare calculated and measured resonance peaks. For this the tested impeller has been provided with a large number of strain gauges.

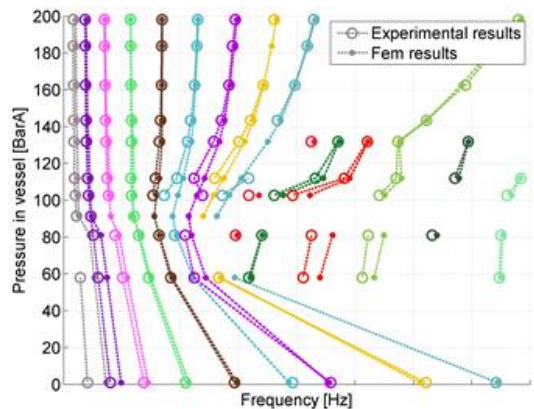


Figure 15 Example of a result of vibration mode identification and comparison with modelling results.

An identification method has been developed with which vibration modes can be identified based on the multi-point strain measurements. A typical result is shown in figure 15.

5. Damping

As in practice excitation of a resonance condition cannot be avoided, the design of a compressor stage should include the response at resonance. At resonance the response is determined by the damping.

In a system with fluid structure coupling the damping of a vibration mode is the result of a combination of acoustic and structural damping. Provided the coupling between fluid and structure is sufficiently strong, the acoustic damping is dominant and the structural damping can be neglected. The structural damping is at least an order of magnitude smaller than the acoustic damping. For the range of 50 to 200 bar CO₂ the coupling is sufficient to make this assumption valid. Therefore the focus is further on the acoustic damping. As mentioned before the BLA model has been applied for acoustic damping.

To verify the structural damping, a test has been done with the “Simple Disk” configuration in air at atmospheric pressure. The FRF measured at this condition, as is shown in figure 16, is very smooth and shows sharp resonance peaks. The structural damping ratio derived from this FRF is in the order of 0.01%, which is at the accuracy limit of the measurement.

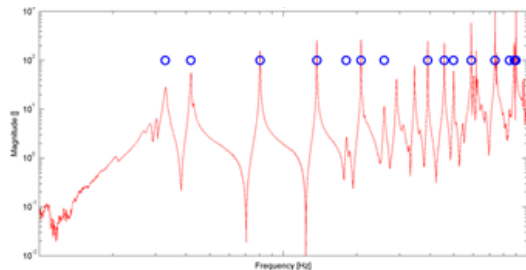


Figure 16 Response of Simple Disk configuration at atmospheric conditions. The blue circles indicate the detected resonance frequencies.

In figure 17 the damping is shown for the same configuration with acoustic-structure coupling. To avoid very long computation times, the damping calculation has been a post processing step after a calculation of the modal response without damping. For this the Boundary Layer

Impedance (BLI) model is used, which is equivalent to the BLA model. The damping calculated in this way, as shown in the upper graph of figure 17, shows clearly a decrease of the damping ratio with increasing frequency and a small increase with increasing pressure. The increase at low pressures is caused by the fact that the damping model is not valid for low pressure.

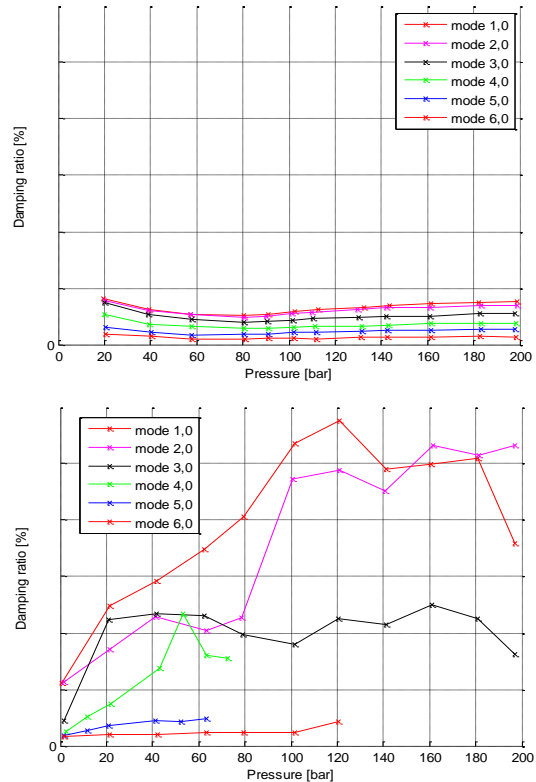


Figure 17 Damping calculated with the BLI model (upper graph) and the damping that has been derived from tests (lower graph).

The measured damping ratio, as is shown in the lower graph of figure 17, show larger values for the damping, also a large decrease with increasing frequency and strong increase with increasing pressure. Further the curves are not smooth. It is supposed that this is caused by measurement inaccuracies.

The large discrepancy between measured and calculated damping has led to the idea that there could be another damping mechanism. A possible additional damping mechanism could be dissipation of acoustic energy at sharp edges by vorticity generation. This can happen for instance

at the rim of the impeller disk and in the narrow clearance between impeller and diffuser. For this mechanism the damping of the acoustic pressure is proportional to the square of the local flow velocity. As there is no mean flow in this case, the decrease of the acoustic pressure is proportional to the square of the acoustic velocity amplitude. This means a non-linear acoustic resistance, which is approximately a constant times the acoustic velocity amplitude. More details are in the box “Flow related acoustic damping”. It is shown that flow related damping, further called aero-acoustic damping (AAD), is proportional to the density, i.e. increases with pressure, but works only at low frequencies.

Flow related acoustic damping

At low frequencies the acoustic damping can be related to the pressure loss in the flow. The pressure loss of a flow is proportional to the square of the flow:

$$\Delta P = K_w \frac{1}{2} \rho |U| U$$

With K_w the friction coefficient that depends on the geometry of the obstruction in the flow, ρ is the fluid density and U the total flow velocity. As $U = U_{mean} + u'$ the acoustic resistance is:

$$R = d\Delta P/du' = K_w \rho |U|$$

This acoustic damping is non-linear; it depends on the flow. As in many cases the mean flow U_{mean} is large compared to the acoustic velocity u' , the acoustic velocity can be neglected:

$$R \approx K_w \rho |U_{mean}|$$

For zero mean flow the acoustic resistance can be based on the acoustic flow amplitude \hat{u}' :

$$R \approx K_w \rho \hat{u}'$$

Because of the non-linearity also a component with twice the frequency is generated, which we further neglect.

At first glance the acoustic resistance seems to be frequency independent. However, as the dissipation depends on the generation of vorticity and vortices, the above approximation is valid for frequencies much lower than the frequency of vortex formation. The limitation of the frequency can be estimated with the Strouhal number:

$$Sr = \frac{fL}{U} < 1 \rightarrow f < \frac{U}{L}$$

In which L is a dimension which is characteristic for the vortex formation.

Further the acoustic resistance is proportional to the fluid density, thus increases with the pressure.

To evaluate the effect of AAD (aero-acoustic or flow related damping) measurements and calculations have been made for a Simple Disk configuration that has been simplified and equipped with more sensitive measurement equipment. As in COMSOL there is no model for AAD, linear damping has been added to the area of the clearance between disk and diffuser. The BLA damping in the clearance has been adjusted such that the equivalent dynamic pressure loss is generated. This means that a certain acoustic velocity amplitude in the clearance has to be assumed that depends on the magnitude of the excitation and the acoustic mode shapes. As a guess two constant velocity amplitudes have been assumed: 0.1 and 1 m/s, identified as AAD respectively AAD+.

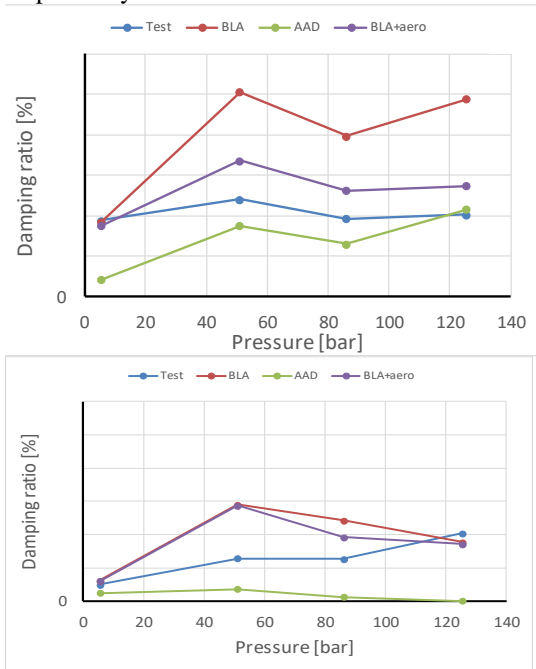


Figure 18 Comparison of various combinations of damping models with measured damping. Upper graph for a low frequency mode, lower graph for a high frequency mode.

For various combinations of damping models a calculation has been made for one specific low frequency (around 150 Hz) and a high frequency (around 800 Hz) resonance peak as well as for 4 mean pressures. The results are summarized in figure 18 for a number of damping models. The upper graph for low frequency (~150 Hz) and the lower graph for a high frequency (~800 Hz).

From figure 18 it appears that the damping is lower for higher frequencies. Also it appears that the BLA model alone gives too high damping. The AAD alone gives too low damping. The combination of BLA and AAD seems to give the best result. The damping for $\hat{u}' = 1 \text{ m/s}$ appears to be high and is left out of the comparison in figure 18.

Although the way in which the non-linear AAD damping is treated is rather crude, it seems that the trends in the calculated damping comply with the trend in the measured damping. However, to draw a final conclusion fine tuning of the damping model parameters and an analysis of all resonance peaks for all pressures is required.

At present a calculation for one frequency peak and for one pressure takes already very much computation time. Therefore a full range analysis is practically impossible. Finally it will be required to implement an AAD model which requires to develop a way to handle non-linearities.

6. Conclusions and remarks

The acoustic structural response of a disk in a narrow space can be calculated accurately with a coupled acoustic and structural model. The resonance frequencies and mode shapes are accurately predicted including the change of these parameters with the pressure (and density) of the gas.

We did not succeed to determine the damping ratio from the complex eigen values. To determine the damping a time consuming response calculation by direct integration had to be applied.

Measured and calculated damping calculated by the BLI model do not comply. An additional damping mechanism seems to contribute. The generation of vorticity in the clearance between impeller disk and diffuser can possibly explain the differences. This type of damping, called 'flow related' or 'Aero Acoustic' damping (AAD) is non-linear and is not implemented in COMSOL. Further analysis is required before it can finally be concluded that AAD is a damping mechanism that should be included in the analysis of the dynamic behavior of a centrifugal compressor stage.

If AAD is an important contribution to the overall damping, it will be the dominant damping in case

there is a mean flow present. This is always the case in a real compressor stage.

7. References

- [1] N. González Díez, J.P.M. Smeulers, F. Moyroud, K. Ramakrishnan, Aero-Acoustic Analysis of a Low-Pressure Centrifugal Compressor Stage, Proceedings of the 13th European Fluid Machinery Congress, 3–4 October 2016, The Hague, Netherlands.
- [2] H.P. Pereboom, P.J.G. van Beek, J.P.M. Smeulers, Experimental Investigation of Fluid Structure Interaction of Impeller Like Disks in Super Critical Carbon Dioxide, GT2016-58032, Proceedings of ASME Turbo Expo 2016, June 13-17, 2016, Seoul, South Korea.
- [3] Azijli, I., Dwight, R.P. Vibro-Acoustic Properties of a Gas-Enclosed Disk under High-Pressure, High-Density Conditions: an Experimental and Numerical Parametric Study, ICEDyn 2015, paper 57, International Conference on Structural Engineering Dynamics, 22-24 June 2015, Lagos, Algarve, Portugal.